MISSOURI S&T

Missouri University of Science and Technology

Scholars' Mine

Geosciences and Geological and Petroleum Engineering Faculty Research & Creative Works

Geosciences and Geological and Petroleum Engineering

01 May 2002

Mantle Discontinuities beneath Southern Africa

Stephen S. Gao
Missouri University of Science and Technology, sgao@mst.edu

Paul G. Silver

Kelly H. Liu
Missouri University of Science and Technology, liukh@mst.edu

Kaapvaal Seismic Group

Follow this and additional works at: https://scholarsmine.mst.edu/geosci_geo_peteng_facwork

Part of the Geology Commons

Recommended Citation

Mantle discontinuities beneath Southern Africa

Stephen S. Gao,[1,2] Paul G. Silver,[3] Kelly H. Liu,[1] and the Kaapvaal Seismic Group[4]

[1]   Seismic velocity discontinuities within the top 1000 km of the Earth beneath southern Africa are imaged by stacking about 1300 source-normalized broadband seismograms recorded by the Southern African Seismic Experiment. The Moho, 410, and 660 kilometer discontinuities are clearly detected. The mean mantle transition zone thickness is 245 km, essentially the same as the global average, suggesting that the transition zone is not anomalously warm. Thus, the lower-mantle 'African Superplume' beneath our study area has no discernible effect on transition zone temperature and is consequently confined to the lower mantle. Variations in transition zone thickness appear to be related to the presence or absence of thick lithosphere. We do not detect several previously-reported discontinuities beneath continents, such as the Hales or Lehmann discontinuities, and find no evidence for a 520 km discontinuity, nor do we detect a previously proposed low-velocity zone just above the transition zone.   *INDEX TERMS:* 7218 Seismology: Lithosphere and upper mantle; 7207 Seismology: Core and mantle; 8120 Tectonophysics: Dynamics of lithosphere and mantle—general

1.   Introduction

[2]   Seismic velocity discontinuities reflect abrupt changes in composition, mineralogy, temperature, or mantle fabric as a function of depth. They consequently mark potentially important layers or structural transitions in the mantle. Some discontinuities are ubiquitous, such as the Moho, and the 410 and 660 kilometer discontinuities (hereafter referred to as $d410$ and $d660$). In addition, the existence of other seismic discontinuities has been reported specifically beneath continental regions, such as the Hales (H) at 80 km [*Hales*, 1969], thought to mark either a phase change from spinel to garnet, or a thin anisotropic layer [*Bostock*, 1998]; the Lehmann discontinuity (L) at 200 km, a possible change from anisotropic to isotropic mantle [*Karato*, 1992; *Gaherty and Jordan*, 1995]; and the bottom of the lithosphere [*Vinnik et al.*, 1996]. In addition, there may be relict structures associated with the continental formation, such as dipping ancient oceanic slabs [*de Wit et al.*, 1992; *Bostock*, 1998], or seismic discontinuities associated with petrological boundaries, such as that separating low-temperature and high-temperature kimberlite nodules, previously thought to represent the lithosphere-asthenosphere boundary [*Boyd and Gurney*, 1986]. With the unprecedented high quality and volume of broadband seismic data from the Southern African Seismic Experiment, we are in an ideal position to characterize the discontinuity structure beneath southern Africa.

[3]   An important parameter derived from $d410$ and $d660$ is mantle transition zone thickness, h_{tz}, defined as the difference in the depths of $d660$ and $d410$, since it is a measure of transition zone temperature. The phase boundaries thought to produce $d410$ and $d660$ have positive and negative Clayperon slopes, respectively, and thus variations in transition-zone thickness can be interpreted as variations in temperature, corresponding to approximately $-6°$/km [e.g., *Revenaugh and Jordan*, 1991]. We are consequently in a position to assess the possible influence of the well-documented lower-mantle low-velocity anomaly beneath Africa [e.g., *Ritsema and Helmberger*, 1998] on the southern African transition zone. For one particular cratonic domain, the Slave Province of the Canadian Shield in North America, at least three mantle discontinuities above the transition zone have been reported, based on P-to-S converted phases [*Bostock*, 1997, 1998]: H (80 km), L (200 km), and an additional discontinuity at 135 km depth. At least two of these have been interpreted as anisotropic discontinuities due to their behavior as a function of backazimuth and the presence of significant energy on the transverse component. We can determine whether there are analogous structures beneath the Kaapvaal craton.

2.   Data and Method

[4]   In this study we use P-to-S conversions to image the discontinuity structure within the top 1000 km beneath southern Africa. The dataset consists of approximately 1300 three-component seismograms for the epicentral distance range of 30° to 100° from 80 broadband transportable stations deployed as part of the Southern African Seismic Experiment, augmented by a 35-station dense broadband array deployed in the Kimberly area (Figure 1). The seismograms are from nearly 200 teleseismic events, which cover a broad back-azimuthal range and provide an excellent distribution in epicentral distance (Figures 1 and 2). The seismograms are converted into radial and transverse receiver functions using the procedure of *Ammon et al.* [1990]. Figure 1 shows station- and event-locations and P-wave ray piercing points at 660 km depth.

[5]   In Figure 2 the receiver functions are grouped into one-degree bins according to their focal-depth-corrected epicentral distances, and those in the same bins are then stacked in the time domain. Several clear arrivals can be observed on the radial component. Using the terminology of *Clarke and Silver* [1991], these arrivals follow the predicted arrival times of the Moho phases $P\dot{m}S$ (about 6 s), $PP\dot{m}S$ (16 s), and $PS\dot{m}S$ (21 s), as well as the conversions from $d410$ and $d660$, termed $P\acute{4}S$ and $P\acute{6}S$, respectively. $P\acute{4}S$ and $P\acute{6}S$ are earlier than the predictions from IASP91 [*Kennett and Engdahl*, 1991], corresponding to estimates of $d410$ = 396 km and $d660$ = 641 km (Figure 3). This implies either that the discontinuities are shallower than in IASP91, or that upper-mantle velocities are higher than this model by about 3.5%. Estimates of upper-mantle velocity from these data [*James et al.*, 2001; *Freybourger et al.*, 2001] suggest that the latter is more likely. We also examined transverse component receiver functions, binning in narrow back-azimuth bands and using stations within the same tectonic regions. We did not, however, detect any clear converted phases on the transverse component, either for the network or the Kimberly broadband array. This rules out the presence of strong anisotropic discontinuities, or discontinuities with significant lateral heterogeneity. In order to calibrate the resolving power of our data processing scheme, we applied it to the Yellowknife-array dataset used in the Bostock studies noted above. We obtained the same upper-mantle arrivals reported in those studies: namely strong transverse-component energy at 80 (H),

[1]Kansas State University, Manhattan, KS, USA.
[2]Formerly at Carnegie Institution of Washington, DC, USA.
[3]Carnegie Institution of Washington, DC, USA.
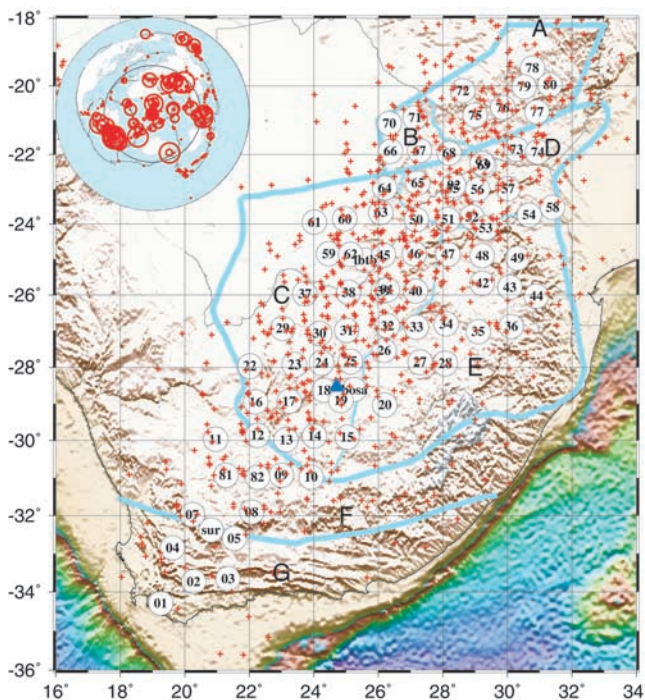[4]http://www.ciw.edu/kaapvaal.

Figure 1. Map showing stations used in the study (circles) and ray piercing point locations at 660 km depth (crosses). The inset at the top-left corner shows the location of the events used in the study. The size of the circles is proportional to the number of teleseismic P-wave records used from the event. The blue triangle gives location of the 35-station Kimberly broadband array. Lines show major geological subdivisions. Also shown are locations of $2° \times 2°$ blocks for the study of spatial variations of discontinuities (see Figure 4). See *Silver et al.* [2001] for description of geologic regions.

135, and 200 (L) km depth, as well as the lateral variations detected in L.

3. Global Stacking

[6] We next stacked all receiver functions for the purpose of detecting possible discontinuities and for estimating sharpness. We first filtered the seismograms in several frequency bands, computed receiver functions, and then stacked the arrivals on the predicted arrival time of the P$\acute{d}$S phase at a range of candidate depths [*Dueker and Sheehan*, 1998] from the surface to 1000 km depth. The predicted arrival time is calculated using the method of *Dueker and Sheehan* [1998] under the assumption that the ray parameters for P and P$\acute{d}$S phases are the same, corresponding to the plane-wave approximation.

[7] Figure 3a shows the results of stacking all the high-quality receiver functions for a sequence of frequency bands. Not surprisingly, the most significant discontinuities are the Moho, d410, and d660. The apparent discontinuities at about 130 km (positive polarity) and 180 km depth (negative polarity) are $PP\check{m}S$ and $PS\check{m}S$, respectively. As shown in Figure 2, they can be distinguished from true P-to-S conversions based on moveout. In order to further assess the effect of Moho reflections, we generated synthetics using the CORE (Complete Ordered Ray Expansion) method [*Clarke and Silver*, 1991; *Clarke*, 1993] for a model with a Moho at 35 km depth for a profile of stations covering the observed range of distances, and for an observed range of event depths. These were then filtered and stacked like the data. We note the similarity between the data and synthetics above 250 km depth,

suggesting that the Moho alone can account for the observed signal in this depth range (Figure 3b).

[8] The average thickness of the mantle transition zone, $\bar{h}_{tz}$, is 245 km, a result that is insensitive to frequency. This value is essentially the same as the global average found by *Flanagan and Shearer* [1998] and *Gu et al.* [1998] of 242 km and 243 km, respectively, using SS precursors. This suggests that the transition zone temperature beneath southern Africa is not anomalous.

[9] The first order discontinuities, the Moho, d410, and d660, can be observed in all the frequency bands below 0.25 Hz. d410 can also be observed in the frequency band $0.5-5.0$ Hz, implying that its thickness is no more than about 8 km based on the assumption that the discontinuity must be thicker than 1/2 of P-wavelength to be observed [*Bostock*, 1999], and d660 is not thicker than about 16 km. These estimates should actually be regarded as upper bounds, because the plane-wave approximation, noise, as well as lateral heterogeneity, will tend to degrade the stack at higher frequencies.

4. Spatial Variations

[10] We next examined spatial variations in d410 and d660 and any other candidate discontinuities by stacking seismograms with ray piercing points in the same $2° \times 2°$ blocks. We find that the Moho is deepest beneath the Limpopo mobile belt (region D in Figure 1) and the off-craton orogenic belts to the southwest (regions F and G, Figure 1), consistent with the results of *Nguuri et al.* [2001]. The stacked radial receiver functions for the blocks are shown in Figure 4. The thinnest transition zone is found beneath the off-craton region to the southwest, where the African
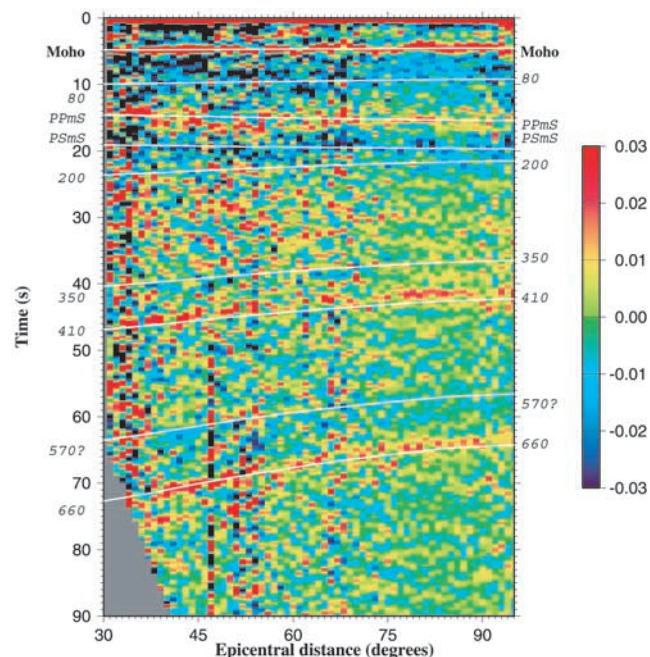

Figure 2. Binned and stacked radial receiver functions. Receiver functions are binned according to their focal-depth-corrected epicentral distances into 1° bins and those in the same bins are then stacked. The purple lines are predicted moveout curves for P$\acute{d}$S phases from discontinuities at 35, 410, and 660 km, other previously proposed or possible discontinuities (80, 200, 350, 570 km), as well as two Moho reverberation phases, $PP\check{m}S$ and $PS\check{m}S$, based on IASP91. Note that the Moho, d410, and d660 are clearly observed, as are $PP\check{m}S$ and $PS\check{m}S$. No other interaction phases can be observed, except possibly at 570 km. Amplitudes are normalized to P-wave amplitudes on radial receiver functions.

lithosphere is relatively thin [*James et al.*, 2001]. The variation between on- and off-craton thickness is about 10 km, which would translate to a temperature difference of 60°C. We note that such a difference could be explained by the effect of a reduction in upper-mantle temperature expected for this lithospheric difference [e.g., *Gu et al.*, 1998].

5. Discussion

[11] There are several features of the discontinuity structure beneath southern Africa that merit further discussion. First, the fact that the transition zone is not anomalously thin strongly suggests that the large-scale seismic velocity anomaly in the lower mantle
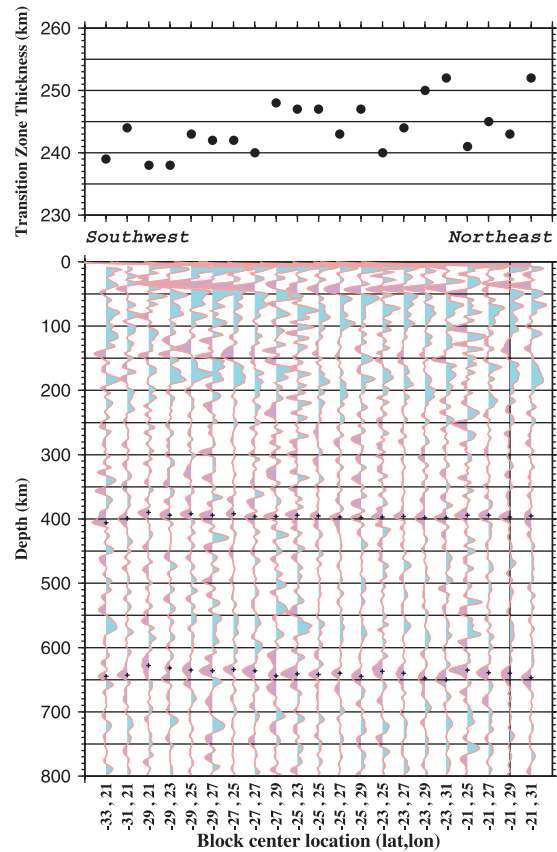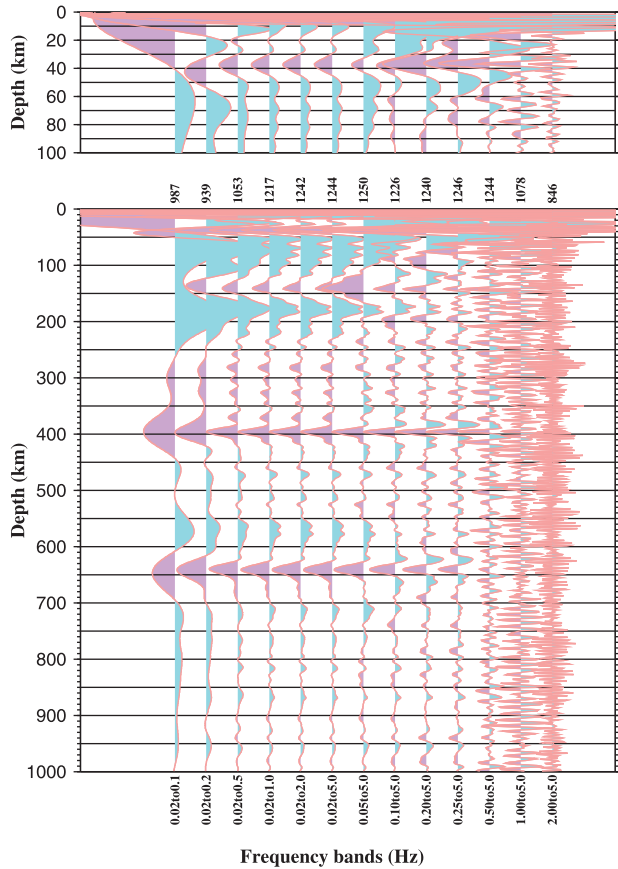

Figure 4. (a) Stacked receiver functions (bottom), and transition zone thicknesses (top) for the 2° × 2° blocks (Figure 1). Positive (negative) polarities are shaded in purple (blue). The geographic coordinates of the center of the blocks are labeled at the bottom of the figure. Note gradual thinning of transition zone to the southwest.

directly beneath our study area (the so-called African Super-plume) has not perturbed the transition zone, and is therefore restricted to the lower mantle. Given the high seismic velocities in the upper mantle and our result for the transition zone, it strengthens the hypothesis that the African superswell is due
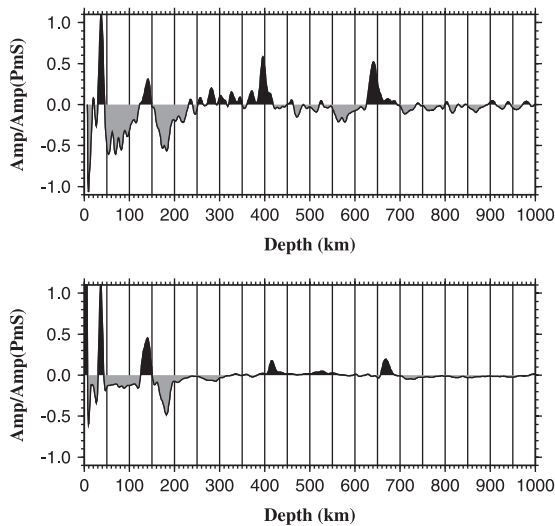
Figure 3. (opposite) (a) The bottom plot shows depth phase images for the entire study area for a sequence of frequency bands. Bands are labeled at bottom of the plot. Positive (negative) polarities are shaded in purple (blue). The traces are normalized by the maximum positive amplitude in the depth range from 350 to 450 km. The number of traces included in the stack is shown at the top of the figure. Note consistency and visibility of d410 and d660 even to relatively high frequencies. The top plot is an enlargement of the top 100 km. (b) The top plot shows images for the frequency band .02−1 Hz. Main peaks are at 35, 396, and 641 km, and artifacts due to Moho reverberation (positive and negative peaks at 135 km and 180 km, respectively). The bottom plot shows images generated using CORE synthetics based on a model that includes the Moho, d410, d660, and the CMB. The model was created by eliminating the other discontinuities in the IASP91 earth model. Traces in (top) and (bottom) were normalized by the amplitude of $P\acute{m}S$. Note that because the Moho depth in the real data (top) varies spatially and that in the synthetic (bottom) is constant, the amplitude of $P\acute{m}S$ is smaller on the top plot than that on the bottom one. This leads to apparent larger amplitudes of $P4S$ and $P6S$ on the top plot.

primarily to dynamic topography induced by this lower mantle anomaly [*Lithgow-Bertelloni and Silver*, 1998]. Second, the absence of a detectable discontinuity between *d*410 and the Moho is surprising, given the high-quality, abundant broadband data available, and the variety of continental discontinuities that have been observed or proposed for other continental regions. This conclusion is based on a careful examination of each of the 2° × 2° regions in Figure 4, a separate stack of the data from the Kimberly array, and an examination of S-to-P conversions for the array as well as the entire dataset. One discontinuity that has been specifically proposed for the Kaapvaal craton corresponds to a velocity decrease at about 350 km depth [*Vinnik et al.*, 1996], based on a much smaller dataset of 43 records. We find, however, no evidence for it, and the interpretation of this hypothesized velocity decrease, namely the presence of partial melt, is not consistent with the 'normal' transition-zone temperatures inferred from h_{tz}.

[12] Why is Kaapvaal upper-mantle discontinuity structure so simple compared to the Slave craton? The strength of anisotropy may be the primary reason. As discussed by *Bostock* [1998], the mantle discontinuity structure beneath the Slave craton primarily represents changes in anisotropic structures, and thus the ability to detect these boundaries is linked to the strength of mantle anisotropy. It is now clearly established that the southern African upper mantle is characterized by particularly weak anisotropy [*Silver et al.*, 2001]. Shear wave splitting analysis reveals that the mean splitting delay time $\overline{\delta t}$ is about 0.6 s where splitting could be detected, and 25% of the stations did not have detectable splitting at all ($\delta t < 0.25$ s). This is well below the continental average of about 1.0 s [*Silver*, 1996]. In contrast, the Slave craton is highly anisotropic with $\overline{\delta t} = 1.2$ s [*Bank et al.*, 2000], more than double that obtained for southern Africa. The overall weak anisotropy beneath the Kaapvaal craton appears to have several reasons, but it is clear from southern African mantle nodules [*Ben-Ismail et al.*, 2001], both on and off craton, that there is an unusual fabric that produces intrinsically weak anisotropy. Thus, the simple character of the southern African upper mantle may be tied to the process that produced this unusual fabric.

[13] Finally, we have used this dataset to search for weaker discontinuities in the top 1000 km of the mantle. We find no sign of a 520 km discontinuity. Our conclusion is consistent with a global study using SS precursors [*Gu et al.*, 1998] that detected it beneath oceanic regions but not beneath shields, such as southern Africa. The strongest and most consistent feature we do observe is a negative arrival at about 570 km (Figure 3). It is seen in several distinct frequency bands and its existence is also suggested in Figure 2. Careful evaluation of these second-order features and possible discontinuities in the mantle below 1000 km is the subject of a subsequent report.

References

Ammon, C. J., G. E. Randall, and G. Zandt, On the non-uniqueness of receiver function inversions, *J. Geophys. Res.*, 95, 15,303–15,318, 1990.

Bank, C. G., M. G. Bostock, R. M. Ellis, and J. F. Cassidy, A reconnaissance teleseismic study of the upper mantle and transition zone beneath the Archean Slave craton in NW Canada, *Tectonophysics*, 319, 151–166, 2000.

Ben-Ismail, W., G. Barruol, and D. Mainprice, The Kaapvaal craton seismic anisotropy: A petrophysical analysis of upper mantle kimberlite nodules, *Geophys. Res. Lett.*, 28, 2497–2500, 2001.

Bostock, M. G., Anisotropic upper-mantle stratigraphy and architecture of the Slave craton, *Nature*, 390, 392–395, 1997.

Bostock, M. G., Mantle stratigraphy and evolution of the Slave province, *J. Geophys. Res.*, 103, 21,183–21,200, 1998.

Bostock, M. G., Seismic waves converted from velocity gradient anomalies in the Earth's upper mantle, *Geophys. J. Int.*, 138, 747–756, 1999.

Boyd, F. R., and J. J. Gurney, Diamonds and the African lithosphere, *Science*, 232, 472–477, 1986.

Clarke, T. J., The complete ordered ray expansion—I. Calculation of synthetic seismograms, *Geophys. J. Int.*, 115, 421–434, 1993.

Clarke, T. J., and P. G. Silver, A procedure for the systematic interpretation of body wave seismograms I. Application to Moho depth and crustal properties, *Geophys. J. Int.*, 104, 41–72, 1991.

de Wit, M., C. Roering, R. H. Hart, R. A. Armstrong, C. E. J. de Ronde, R. W. Green, M. Tredoux, E. Peberdy, and R. A. Hart, Formation of an Archean continent, *Nature*, 357, 553–562, 1992.

Dueker, K. G., and A. F. Sheehan, Mantle discontinuity structure beneath the Colorado Rocky Mountains and High Plains, *J. Geophys. Res.*, 103, 7153–7169, 1998.

Flanagan, M. P., and P. M. Shearer, Global mapping of topography on transition zone velocity discontinuities by stacking SS precursors, *J. Geophys. Res.*, 103, 2673–2692, 1998.

Freybourger, M., J. B. Gaherty, T. H. Jordan, and the Kaapvaal Seismic Group, Structure of the Kaapvaal craton from surface waves, *Geophys. Res. Lett.*, 28, 2489–2492, 2001.

Gaherty, J. B., and T. H. Jordan, Lehmann discontinuity as the base of an anisotropic layer beneath continents, *Science*, 268, 1468–1471, 1995.

Gu, Y., A. M. Dziewonski, and C. B. Agee, Global de-correlation of the topography of transition zone discontinuities, *Earth Planet. Sci. Lett.*, 157, 57–67, 1998.

Hales, A. L., A seismic discontinuity in the lithosphere, *Earth Planet. Sci. Lett.*, 7, 44–46, 1969.

James, D. E., M. J. Fouch, J. C. VanDecar, S. van der Lee, and the Kaapvaal Seismic Group, Tectospheric structure beneath southern Africa, *Geophys. Res. Lett.*, 28, 2485–2488, 2001.

Karato, S., On the Lehmann discontinuity, *Geophys. Res. Lett.*, 19, 2255–2258, 1992.

Kennett, B. L. N., and E. R. Engdahl, Travel times for global earthquake location and phase identification, *Geophys. J. Int.*, 105, 429–465, 1991.

Lithgow-Bertelloni, C., and P. G. Silver, Dynamic topography, plate driving forces, and the African superswell, *Nature*, 395, 269–272, 1998.

Nguuri, T. K., J. Gore, D. E. James, S. J. Webb, C. Wright, T. G. Zengeni, O. Gwavava, J. A. Snoke, and the Kaapvaal Seismic Group, Crustal structure beneath southern Africa and its implications for the formation and evolution of the Kaapvaal and Zimbabwe cratons, *Geophys. Res. Lett.*, 28, 2501–2504, 2001.

Revenaugh, J., and T. H. Jordan, Mantle layering from ScS reverberations; 2, The transition zone, *J. Geophys. Res.*, 96, 19,763–19,780, 1991.

Ritsema, J., S. Ni, and D. V. Helmberger, Evidence for strong shear velocity reductions and velocity gradients in the lower mantle beneath Africa, *Geophys. Res. Lett.*, 25, 4245–4248, 1998.

Silver, P. G., Seismic anisotropy beneath the continents: Probing the depths of geology, *Annu. Rev. Earth Planet. Sci.*, 24, 385–432, 1996.

Silver, P. G., S. S. Gao, K. H. Liu, and the Kaapvaal Seismic Group, Mantle deformation beneath southern Africa, *Geophys. Res. Lett.*, 28, 2493–2496, 2001.

Vinnik, L. P., R. W. E. Green, L. O. Nicolaysen, G. L. Kosarev, and N. V. Petersen, Deep seismic structure of the Kaapvaal craton, *Tectonophysics*, 262, 67–75, 1996.

———————————
S. S. Gao and K. H. Liu, Department of Geology, Kansas State University, Manhattan, KS 66506, USA. (sgao@ksu.edu; liu@ksu.edu)

P. G. Silver, Department of Terrestrial Magnetism, Carnegie Institution of Washington, 5241 Broad Branch Road, N.W., Washington, DC 20015, USA. (silver@dtm.ciw.edu)

Kaapvaal Seismic Group, http://www.ciw.edu/kaapvaal.